

Measurement of helium-like and hydrogen-like argon spectra using double-crystal X-ray spectrometers on EAST

B. Lyu, J. Chen, R. J. Hu, F. D. Wang, Y. Y. Li, J. Fu, Y. C. Shen, M. Bitter, K. W. Hill, L. F. Delgado-Aparicio, N. Pablant, S. G. Lee, M. Y. Ye, Y. J. Shi, and B. N. Wan

Citation: [Review of Scientific Instruments](#) **87**, 11E326 (2016); doi: 10.1063/1.4960504

View online: <http://dx.doi.org/10.1063/1.4960504>

View Table of Contents: <http://aip.scitation.org/toc/rsi/87/11>

Published by the [American Institute of Physics](#)

Articles you may be interested in

[Upgrades of poloidal and tangential x-ray imaging crystal spectrometers for temperature and rotation measurements on EAST](#)

[Review of Scientific Instruments](#) **87**, 11E34211E342 (2016); 10.1063/1.4963150

[Upgrades of imaging x-ray crystal spectrometers for high-resolution and high-temperature plasma diagnostics on EAST](#) Contributed paper, published as part of the Proceedings of the 20th Topical Conference on High-Temperature Plasma Diagnostics, Atlanta, Georgia, USA, June 2014.

[Review of Scientific Instruments](#) **85**, 11E40611E406 (2014); 10.1063/1.4886387

[Measurement of the electron and ion temperatures by the x-ray imaging crystal spectrometer on joint Texas experimental tokamak](#) Contributed paper, published as part of the Proceedings of the 21st Topical Conference on High-Temperature Plasma Diagnostics, Madison, Wisconsin, USA, June 2016.

[Review of Scientific Instruments](#) **87**, 11E31811E318 (2016); 10.1063/1.4960060

[First measurement of the edge charge exchange recombination spectroscopy on EAST tokamak](#) Contributed paper, published as part of the Proceedings of the 21st Topical Conference on High-Temperature Plasma Diagnostics, Madison, Wisconsin, USA, June 2016.

[Review of Scientific Instruments](#) **87**, 11E50111E501 (2016); 10.1063/1.4955279

[Electron density profile measurements from hydrogen line intensity ratio method in Versatile Experiment Spherical Torus](#)

[Review of Scientific Instruments](#) **87**, 11E54011E540 (2016); 10.1063/1.4960535

Applied Physics Reviews

SAVE THE DATE!

3D Bioprinting: Physical and Chemical Processes

May 2–3, 2017 • Winston Salem, NC, USA

Measurement of helium-like and hydrogen-like argon spectra using double-crystal X-ray spectrometers on EAST

B. Lyu,^{1,2,a)} J. Chen,^{1,3} R. J. Hu,^{1,3} F. D. Wang,¹ Y. Y. Li,¹ J. Fu,¹ Y. C. Shen,^{1,4} M. Bitter,⁵ K. W. Hill,⁵ L. F. Delgado-Aparicio,⁵ N. Pablant,⁵ S. G. Lee,⁶ M. Y. Ye,³ Y. J. Shi,^{2,7} and B. N. Wan¹

¹*Institute of Plasma Physics, Chinese Academy of Sciences, Hefei 230031, China*

²*Hefei Science Center, Chinese Academy of Sciences, Hefei 230031, China*

³*School of Nuclear Science and Technology, University of Science and Technology of China, Hefei 230026, China*

⁴*School of Physics and Electronic Engineering, Anqing Normal University, Anqing 246011, China*

⁵*Princeton Plasma Physics Laboratory, Princeton, New Jersey 08543, USA*

⁶*National Fusion Research Institute, Daejeon 305-333, South Korea*

⁷*Department of Nuclear Engineering, Seoul National University, Seoul 151-742, South Korea*

(Presented 8 June 2016; received 4 June 2016; accepted 18 July 2016; published online 18 August 2016)

A two-crystal assembly was deployed on the tangential X-ray crystal spectrometer to measure both helium-like and hydrogen-like spectra on EAST. High-quality helium-like and hydrogen-like spectra were observed simultaneously for the first time on one detector for a wide range of plasma parameters. Profiles of line-integrated core ion temperatures inferred from two spectra were consistent. Since tungsten was adopted as the upper divertor material, one tungsten line (W XLIV at 4.017 Å) on the short-wavelength side of the Lyman- α line ($L\alpha 1$) was identified for typical USN discharges, which was diffracted by a He-like crystal ($2d = 4.913$ Å). Another possible Fe XXV line (1.85 Å) was observed to be located on the long-wavelength side of resonance line (w), which was diffracted from a H-like crystal ($2d = 4.5622$ Å) on the second order. Be-like argon lines were also observable that fill the detector space between the He-like and H-like spectra. *Published by AIP Publishing.* [<http://dx.doi.org/10.1063/1.4960504>]

I. INTRODUCTION

Recently, the tangential X-ray spectrometer was developed to contain two crystals and extend the system's capability for diagnosing high-temperature plasmas with upgraded auxiliary heating powers on EAST.¹ Utilizing the width of newly deployed large-area solid X-ray detector, high-quality hydrogen-like and helium-like argon spectra were recorded simultaneously for the same discharge. Additionally, a two-crystal setup also allowed more line emission from other impurities such as W, Mo, and Fe to be diffracted and mix with the argon spectra. This paper reports the newest experimental results from the two-crystal spectrometer and representative spectra containing other impurity lines on EAST to illustrate the complexity of two-crystal spectra used for plasma diagnostics.

II. SIMULTANEOUS MEASUREMENT OF He-LIKE AND H-LIKE ARGON SPECTRA

The selection of crystal type and geometric parameters such as the radius of curvature was determined such that the Bragg angles for He-like and H-like spectra were close enough

to fit two spectra on one detector. Table I summarized the parameters of crystals used on the tangential spectrometer. It could be seen that the chosen crystal types result in similar Bragg angles for He-like and H-like argon spectra. When aligning the detector-to-crystal distance based on the average Bragg angle from two spectra, the recorded spectra are calculated to cover the detector width of ~ 79 mm, which is within the effective detector width (83.8 mm). This indicated that the spectra should be recorded, although part of the spectra may be affected due to the curved shape and Doppler broadening and shift. Experimental measurements also confirmed that the two spectra could be recorded by carefully positioning the detector to fully exploit the detector width.

Lithium was typically applied as one of the main wall conditioning materials on EAST to control and suppress wall influx and impurity accumulation. This also largely prevented contamination of argon spectra from other impurity's line emissions, although molybdenum and tungsten presently cover more than half of the plasma facing surface. Fig. 1 showed time-integrated typical measurement of two argon spectra with effective lithium wall conditioning ($T_{e0} \sim 1.5$ keV). Spatially and spectrally resolved He-like argon spectra at full wavelength range were present and extended towards almost the entire detector length with the strongest intensity found in the center. For H-like spectra, the line intensity was much weaker and only visible in the center region of plasma due to higher excitation energy than He-like spectra. In the space between two argon spectra, there were several lines that were vaguely

Note: Contributed paper, published as part of the Proceedings of the 21st Topical Conference on High-Temperature Plasma Diagnostics, Madison, Wisconsin, USA, June 2016.

^{a)}Author to whom correspondence should be addressed. Electronic mail: blu@ipp.ac.cn.

TABLE I. Crystal choice for the two-crystal spectrometer.

Impurity	Crystal		Wavelength range (Å)	Bragg angle (deg)
	Type	2d (Å)		
Ar XVII	110	4.913 04	3.9494, 3.9944	53.50, 54.39
Ar XVIII	102	4.562 25	3.7300, 3.7353	54.84, 54.95

visible, which were emitted from excited Be-like argon ions. Fig. 2 also plotted a spectrum for a sightline passing through the plasma center. Besides the He-like spectra and two Lyman- α lines from H-like spectra, there were lines emitted from Be-like argon located in the region between He-like and H-like spectra. No significant contamination of spectra by other impurities was observed.

To first validate the H-like spectra measurement, ion temperature profiles inferred from two spectra were analyzed. For typical EAST parameters, argon ion temperatures were expected to agree for two types of spectra. Here, the H-like spectra were simply fitted with two Gaussian functions without taking into account other lines on the short-wavelength side of H-like spectra. This might overestimate the ion temperature slightly. For He-like spectra, ion temperatures were determined by fitting the w line and its neighboring $n \geq 3$ satellites using a Voigt function. Fig. 3 showed the calculated profiles of ion temperatures for a discharge with $I_p \sim 500$ kA, $n_{e0} \sim 2.1 \times 10^{19} \text{ m}^{-3}$ heated with $P_{LHW} \sim 1.2$ MW and $P_{ECRH} \sim 0.5$ MW ($T_{e0} \sim 3.0$ keV). It could be seen that the ion temperature from the two spectra were indeed comparable within uncertainty with the results from H-like spectra higher than He-like spectra in the plasma core. This was expected since the line-integrating effect was more prominent for He-like spectra than H-like ones as the electron temperature increased above 2.5 keV. He-like argon ion density would evolve into a hollow profile while the H-like one remained more peaked due to the vastly different excited rate coefficients at the same electron temperature. However, the preliminary comparison indicated that the two-crystal assembly could produce high-quality spectra for analyzing ion temperature profiles both from He-like and H-like features, as reported on Alcator C-Mod.²

III. OBSERVATION OF OTHER IMPURITY LINES IN THE Ar SPECTRA

In more recent EAST experiments, upper tungsten divertors were further commissioned for high-power auxiliary

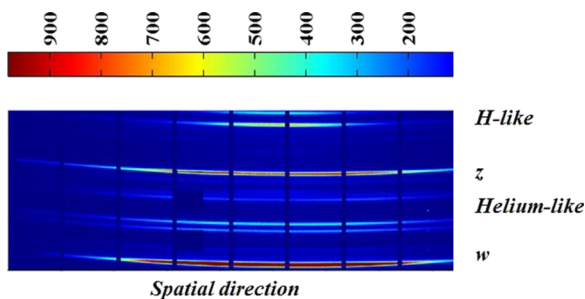


FIG. 1. Spatially and spectrally resolved He-like and H-like spectra measured on EAST.

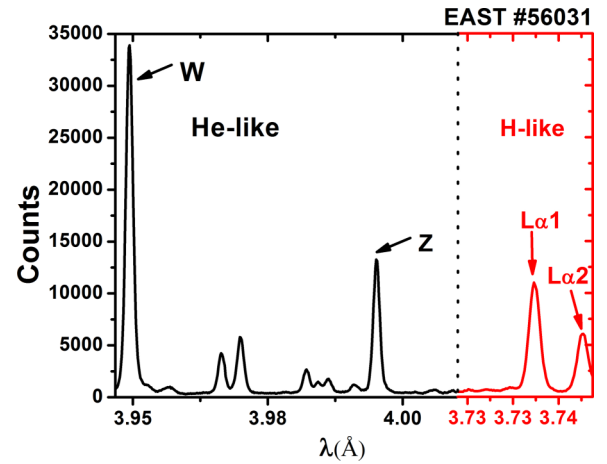


FIG. 2. He-like and H-like spectra observed on the central sightline. The wavelength scale was divided into two parts to illustrate He-like and H-like Ar spectra on one plot.

heating upper-single-null (USN) discharges to take advantage of its high heat handling capability. With concurrently less applied lithium wall conditions, more tungsten ions were expected to accumulate in the plasma. Additionally, Mo and Fe lines were also present due to enhanced plasma-wall interaction associated with higher heating power delivered to the plasma, since Mo is one of the main first-wall materials and Fe is present such as in ICRF antenna. This section presented some spectral measurements from most recent plasma operations showing more lines that were present in the argon spectra that were hardly seen in the discharges with effective lithium wall conditions.

Fig. 4 plotted spectra recorded for an USN diverted plasma ($I_p \sim 360$ kA, $n_{e0} \sim 4.0 \times 10^{19} \text{ m}^{-3}$) heated with $P_{LHW} \sim 1.6$ MW and $P_{ICRH} \sim 1.8$ MW. Here the wavelength ruler was evaluated based on both He-like spectra (bottom) and H-like spectra (top) to help identification of the lines. Two prominent lines were present (labeled as L1 and L2). L1 and L2 were located on the long-wavelength side of the w line and z line, respectively. The wavelength scales were estimated based on the He-like and H-like argon spectra (first or second order) and were searched in NIST Atomic Spectra Database to identify the possible line.³ A preliminary search indicated

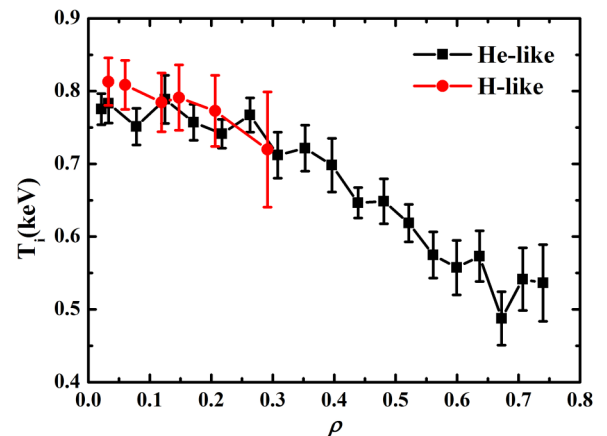


FIG. 3. Comparison of ion temperature profiles inferred from He-like and H-like argon spectra.

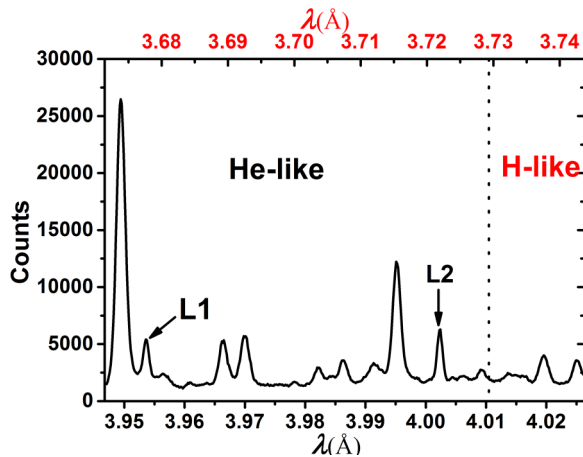


FIG. 4. Sample spectra with lines from other impurities. Note that the bottom scale is based on He-like argon spectra and the top scale is based on H-like argon spectra.

that L1 was mostly likely Mo XXXIII at 3.684 Å diffracted by H-like spectra of the first order.⁴ The roughly estimated value was 3.6894 Å, which was also close to the value of 3.682 Å in Ref. 5. A more accurate wavelength will be determined through spectra fitting taking into consideration Doppler shift from plasma rotation. Additionally, since these two lines were only typically observed for ICRF heated discharge, we surmised that there were possibly diffracted on the second-order of iron lines as the surface of the ICRF antenna was mainly comprised of stainless steel and L2 was similarly determined to be from Fe XXV at 1.8505 Å. To infer correct ion temperature and electron temperature, these lines must be taken into account.

Additionally, a prominent tungsten line was first observed for H-mode USN discharges when heated with counter-current

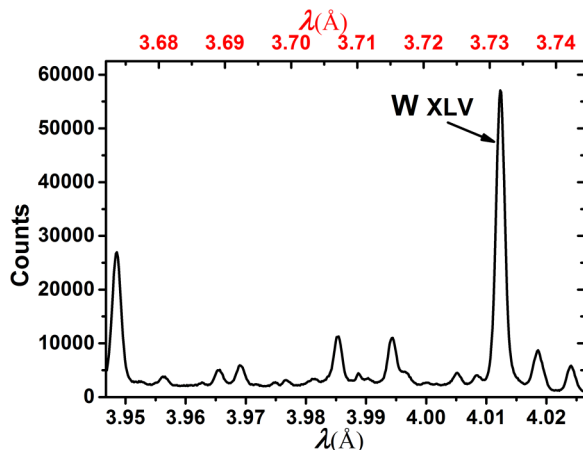


FIG. 5. Two-crystal spectra showing the presence of a strong tungsten line. Note that the bottom scale is based on He-like argon spectra and the top scale is based on H-like argon spectra.

NBI and ECRH. Fig. 5 showed a central-chord spectra from a discharge with $I_p \sim 450$ kA, $n_{e0} \sim 2.6 \times 10^{19} \text{ m}^{-3}$ heated mainly with $P_{LHW} \sim 2.6$ MW and $P_{\text{ctr-NBI}} \sim 1$ MW. The most important feature is that a W XLIV line (4.017 Å) was excited to much higher intensity than the active w line and dominates in the spectra.⁶ The line was identified through wavelength ruler based on He-like and H-like spectra. This was consistent with W impurity accumulation in the core measured by Extreme Ultraviolet (EUV) spectrometer.⁷ As more W entered the plasma core, the intensity also increased and even exceeded the previously strongest argon lines. This discharge ended with disruption due to severe core impurity radiation.

IV. CONCLUSIONS

A two-crystal X-ray spectrometer was successfully commissioned on EAST to extend the system's capability for diagnosing high-temperature plasmas. High-quality He-like and H-like argon spectra were captured and inferred ion temperatures were consistent. With elevated plasma performance and different heating scenarios, more lines from impurities like W, Mo, and Fe were also present in the spectra, affecting the spectral analysis but also providing an opportunity to study tungsten spectra. An important usage will also be explored to using two spectra for absolute wavelength calibration.⁸

ACKNOWLEDGMENTS

The authors wish to thank the EAST team including the diagnostic group, vacuum group, auxiliary heating group, and the operation team for their assistance. The work is partially supported by National Magnetic Confinement Fusion Science Program of China (Grant Nos. 2013GB112004 and 2015GB103002), National Natural Science Foundation of China (Grant Nos. 11175208, 11305212, and 11261140328), Innovative Program of Development Foundation of Hefei Center for Physical Science and Technology (Grant No. 2014FXCX003), and Hefei Science Center of Chinese Academy of Sciences Users with Potential Project (No. 2015HSC-UP007).

¹B. Lyu *et al.*, *Rev. Sci. Instrum.* **85**, 11E406 (2014).

²M. Reinke *et al.*, *Rev. Sci. Instrum.* **83**, 113504 (2012).

³See <http://www.nist.gov/pml/data/asd.cfm> for NIST Atomic Spectra Database version 5.

⁴T. Shirai *et al.*, *J. Phys. Chem. Ref. Data, Monogr.* **8**, 632 (2000).

⁵J. E. Rice *et al.*, *Phys. Rev. A* **51**, 3551 (1995).

⁶N. Tragin *et al.*, *Phys. Scr.* **37**, 79 (1988).

⁷Y. C. Shen *et al.*, *Nucl. Instrum. Methods Phys. Res., Sect. A* **700**, 86 (2013).

⁸M. Bitter *et al.*, in *Proceedings of 27th EPS Conference on Controlled Fusion and Plasma Physics, Budapest, 12-16 June 2000*, Vol. 24B, pp. 840-843.